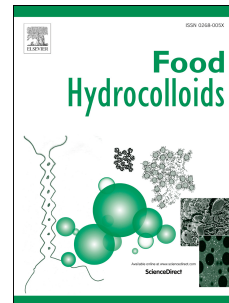


Accepted Manuscript

Interactions between different forms of bovine lactoferrin and sodium alginate affect the properties of their mixtures

Huma Bokkhim, Nidhi Bansal, Lisbeth Grøndahl, Bhesh Bhandari



PII: S0268-005X(15)00002-8

DOI: [10.1016/j.foodhyd.2014.12.036](https://doi.org/10.1016/j.foodhyd.2014.12.036)

Reference: FOOHYD 2839

To appear in: *Food Hydrocolloids*

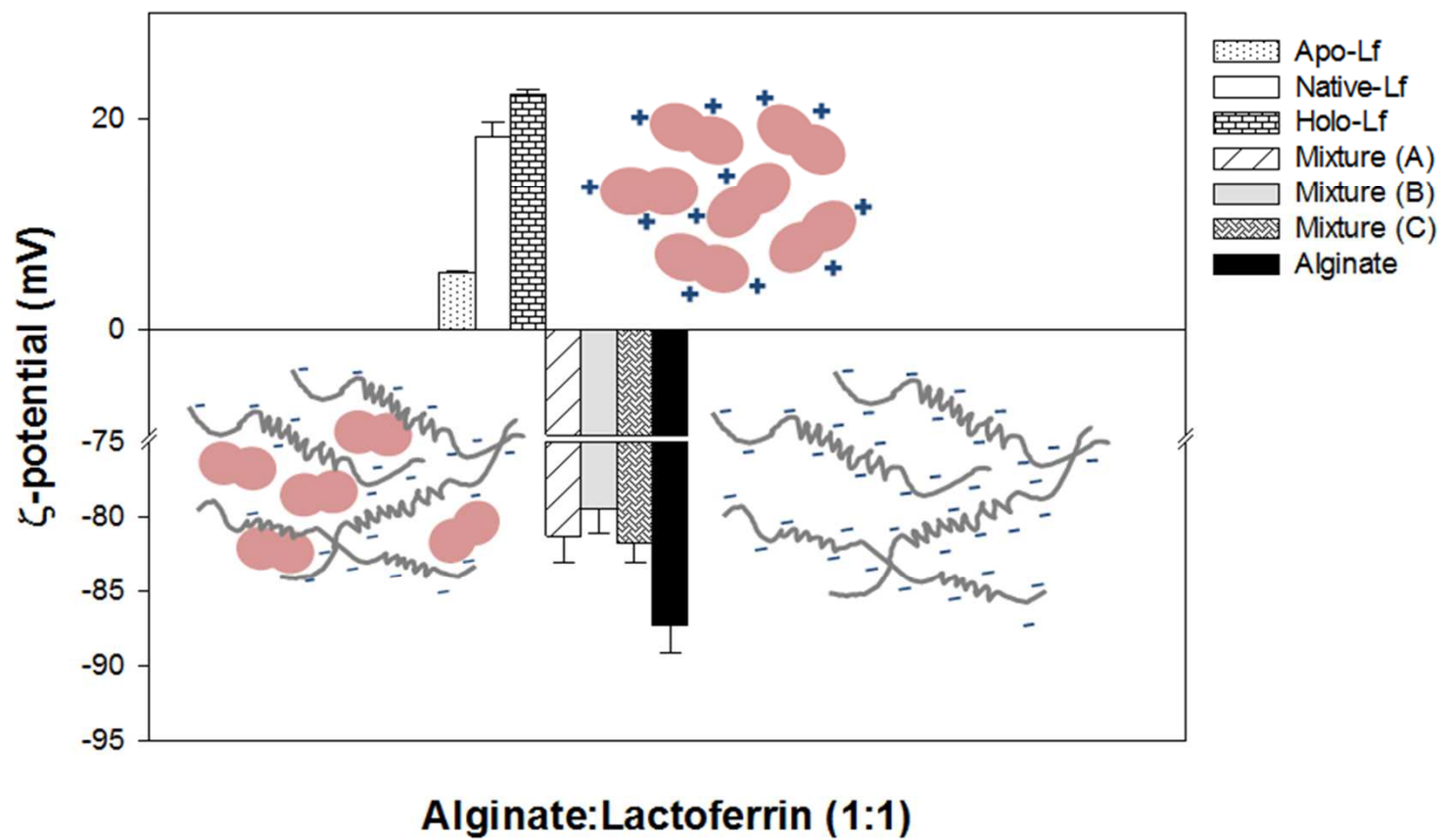
Received Date: 3 November 2014

Revised Date: 29 December 2014

Accepted Date: 31 December 2014

Please cite this article as: Bokkhim, H., Bansal, N., Grøndahl, L., Bhandari, B., Interactions between different forms of bovine lactoferrin and sodium alginate affect the properties of their mixtures, *Food Hydrocolloids* (2015), doi: 10.1016/j.foodhyd.2014.12.036.

This is a PDF file of an unedited manuscript that has been accepted for publication. As a service to our customers we are providing this early version of the manuscript. The manuscript will undergo copyediting, typesetting, and review of the resulting proof before it is published in its final form. Please note that during the production process errors may be discovered which could affect the content, and all legal disclaimers that apply to the journal pertain.



Title Page Information

Title: Interactions between different forms of bovine lactoferrin and sodium alginate affect the properties of their mixtures

Author names and affiliations: Huma Bokkhim^a, Nidhi Bansal^a, Lisbeth Grøndahl^b and Bhesh Bhandari^{a*}

Huma Bokkhim: h.raai@uq.edu.au

Nidhi Bansal: n.bansal@uq.edu.au

^aThe University of Queensland, School of Agriculture and Food Sciences, Brisbane, QLD 4072, Australia

Lisbeth Grøndahl: l.grondahl@uq.edu.au

^bThe University of Queensland, School of Chemistry and Molecular Biosciences, Brisbane, QLD 4072, Australia

*Corresponding author. Address: The University of Queensland, School of Agriculture and Food Sciences, Brisbane, QLD 4072, Australia.

Tel.: +61 7 3346 9192; Fax:

E-mail address: b.bhandari@uq.edu.au

1 **Abstract**

2 The interactions between different forms (apo-, native- and holo-) of lactoferrin (Lf) and
3 sodium alginate at different ratios in aqueous solution in the pH range of 4-7 were evaluated.
4 Fourier transform infra-red (FTIR) spectra of freeze dried mixtures showed shifts only in the
5 bands arising from the carboxylate groups of alginate relative to physical mixtures; indicating
6 intermolecular interactions involving COO⁻ moieties of alginate. Circular dichroism (CD)
7 spectroscopy showed that Lf retained its tertiary structure in the Lf-alginate mixtures. In the
8 pH range of 4 - 7, the zeta-potential of Lf-alginate solutions was significantly less negative
9 than that of alginate indicating charge compensation. Native-PAGE results indicated that the
10 extent of binding of Lf by alginate was dependent of the form of Lf with apo-Lf displaying a
11 higher binding affinity. At natural pH, the Lf-alginate mixtures generated higher viscosities
12 than their respective sodium alginate controls indicating the existence of intermolecular
13 interactions between the two components. A mixture of native-Lf and sodium alginate
14 showed the highest increase in the viscosity while increasing level of iron saturation in Lf
15 showed an inverse effect on viscosity. DSC analysis showed that the thermal denaturation
16 temperature of native- and holo-Lf can be enhanced upon interaction with alginate in
17 solution.

18 **Keywords:**

19 Lactoferrin, sodium alginate, complexation, zeta-potential, viscosity, gel electrophoresis,
20 denaturation temperature

21 **Introduction**

22 Intermolecular interactions, mainly electrostatic interactions between proteins and
23 polysaccharides, are explored in the food and pharmaceutical industries for the development

24 of successful protein delivery systems (Peinado, Lesmes, Andrés & McClements, 2010).
25 These interactions are influenced by the physico-chemical properties of the proteins and
26 polysaccharides as well as environmental factors (pH, ionic strength, protein-to-
27 polysaccharide ratio, temperature and mixing process) and can be manipulated to fabricate
28 protein/polysaccharide complexes with a new set of properties in comparison to the proteins
29 and polysaccharides alone (Benichou, Aserin & Garti, 2002; Schmitt & Turgeon, 2011; Ye,
30 2008). As detailed by Tolstoguzov (1991), the interaction between proteins and
31 polysaccharides may lead to either their co-solubility, incompatibility (phase separation), or
32 complexation (soluble or insoluble). The charges on the proteins/polysaccharides, presence of
33 oppositely charged side groups (acidic and basic) and availability of charged patches in the
34 polyions can play decisive roles in complex formation. Soluble complexes can form when the
35 net charges of proteins and polysaccharides are very different (Ye, 2008).

36 The glycoprotein Lactoferrin (Lf) possesses a broad spectrum of functional properties
37 towards humans and animals such as cellular growth regulation and differentiation, intestinal
38 iron homeostasis, host defense against microbial infection and inflammation, regulation of
39 myelopoiesis, immunomodulatory and anti-oxidant activities and protection against cancer
40 (Conneely & Ward, 2004; Guo, Pan, Rowney, & Hobman, 2007). In order to exploit these
41 benefits, Lf is being increasingly used in health products. However, these functional
42 properties of Lf are affected by different factors during production, storage, transport and
43 consumption such as heat, salts, pH and enzymes (Abe et al., 1991; Naidu, 2006; Steijns,
44 Brummer, Troost, & Saris, 2001; Eriksen et al., 2010, Onishi, 2011). Lf is a cationic protein
45 with positively charged regions most prominently at the N-terminus, as well as in an inter-
46 lobe region between the C- and N-lobes close to a connecting helix (Moore, Anderson,
47 Groom, Haridas, & Baker; 1997) and as such it has a high isoelectric point (pI ~ 8.0-9.0)
48 (Baker, 2005; Brisson, Britten, & Pouliot, 2007, Ye & Singh, 2007; Bokkhim, Bansal,

49 Grøndahl, & Bhandari, 2013). A substantial amount of research on Lf has been conducted by
50 the pharmaceutical sector regarding its biochemical characterization and biological activities.
51 In the food sector, studies have focussed on digestion and thermal stability mostly in Lf's
52 natural form in different food systems. Lately, several researchers have explored Lf's
53 technological properties (emulsifying and stabilizing) in oil-in-water emulsions (Bengoechea,
54 Jones, Guerrero, & McClements, 2011; Bengoechea, Peinado, & McClements, 2011). In
55 order to optimise stability and achieve safe delivery of Lf, its encapsulation in a high heat and
56 acid stable matrix such as alginate is a potential avenue for new product development. The
57 full potential of such a system can be reached only with the detailed knowledge of the
58 intermolecular interactions between Lf and alginate and their effect on the properties of the
59 mixture which can influence the fabrication of a delivery system and the release property of
60 Lf.

61 Sodium alginate is an anionic polysaccharide extracted from the brown algae which is
62 composed of polymeric sequences of (1-4) linked β -D-mannuronate (M) and α -L-guluronate
63 (G) residues (Draget, 2009). Alginate molecules possess ion exchange property because of
64 the presence of the carboxylic groups in both the M and G residues and have a high affinity
65 for di- and tri-valent ions and cationic protein molecules (Zhao, Li, Carvajal, &
66 Harris, 2009). Electrostatic interactions between the negatively charged alginate polymer and
67 positively charged proteins have been studied for lysozyme and chymotrypsin where gelling
68 of the mixtures were observed (Wells & Sheardown, 2007) and for heat treated Lf particles
69 where turbidity, dynamic light scattering and electrophoretic measurements were used to
70 probe effect of pH and ionic strength (Peinado et al., 2010). In addition, alginate has been
71 used to encapsulate vascular endothelial growth factor (Gu, Amsden, & Neufeld, 2004)
72 leading to its sustained release from the alginate matrix. The interactions between the protein
73 and alginate are mainly controlled by the charge density of the protein and the type of

74 alginate used (e.g. M/G ratio, molecular mass) (Turgeon, Schmitt, & Sanchez, 2007). During
75 the process encapsulating a protein, the functional properties of the protein might be altered
76 due to e.g. electrostatic interactions with the alginate matrix (McClements, 2006). It has been
77 reported that with some proteins such as transforming growth factor-beta (TGF- β 1),
78 irreversible complex formation can occur between the protein and alginate molecules
79 resulting in protein inactivation. In such cases additives that protect the protein from the
80 alginate polymer should be added to retain protein activity (Gombotz & Wee, 1998).

81 This study aims to investigate the interactions between different forms of Lf (apo-, native-
82 and holo-) and alginate in aqueous solution at the natural pH of the proteins and in the pH
83 range of 4 to 7. As different forms of Lf demonstrate different physico-chemical properties
84 (Bokkhim et al., 2013), it is important to investigate how those properties affect the
85 intermolecular interactions in the Lf-alginate mixtures. For many application of proteins, it is
86 important to evaluate if the intermolecular interactions in the protein-polyelectrolyte complex
87 affects the secondary and/or tertiary structure and thus functional properties of the protein,
88 and in this study, this was evaluated using Fourier transform infra-red (FTIR) and circular
89 dichroism (CD) spectroscopy. A measure of the binding affinity of different forms of Lf to
90 alginate was evaluated using gel electrophoresis. zeta-potential measurements were done in
91 order to evaluate complex formation and the properties of the mixtures were investigated
92 through the use of viscosity, as well as DSC for the thermal properties of the protein in the
93 mixtures. The research findings will provide fundamental information regarding the potential
94 benefits and application of Lf-alginate mixtures.

95 **Experimental Section**

96 **Materials**

97 Two forms of bovine lactoferrin (NatraFerrin), native- and apo- forms with iron saturation
98 levels approximately 13 and 1% were provided by MG Nutritionals®, Burnswick, Australia.
99 Sodium alginate (PE 12001-13.8 EN), GRINDSTED® Alginate FD 155 (M/G ratio 1.5) was
100 donated by Danisco Australia Pty. Ltd., Sydney, Australia. The molecular mass was
101 determined by U-tube viscometry using and the appropriate Mark-Houwink constant (Vold et
102 al. 2006, Vold et al. 2007) and found to be 140 kDa. Bis (2-hydroxymethyl) iminotris-
103 [hydroxymethyl] methane) (bis-tris) (purity > 98%), potassium chloride, sodium hydroxide,
104 sodium acetate (trihydrate), Trizma® base and glycine were purchased from Sigma Aldrich
105 Co., Castle Hill, Australia (purity > 99 %). Acetic acid (99%), hydrochloric acid
106 (concentration ~ 31.5%) and methanol (99.8%) were from Labtek Pty. Ltd., Brendale,
107 Australia. Sodium dodecyl sulphate (SDS) and glycerol, both of analytical grades were
108 bought from Amresco, Solon, USA and Ajax Finechem Pty. Ltd., Taren Point, Australia
109 respectively. The dyes, bromophenol blue and Coomassie brilliant blue G-250 were from
110 Bio-rad, Gladesville, Australia. Millipore water was used for all experiments. All chemicals
111 used in this study were of analytical grade. Lactoferrin having 50% iron saturation level and
112 holo-Lf were prepared in the laboratory according to the method described by Bokkhim,
113 Tran, Bansal, Grøndahl and Bhandari (2014).

114 **Methods**

115 The Lf-alginate mixtures (2 % w/w) at 1:1 mixing ratio were prepared in Millipore water,
116 allowed to stand at room temperature (22 ± 2 °C) overnight and freeze dried (Christ, ALPHA
117 1-4 LSC, Osterode, Germany). Control samples of dry mixed Lf and alginate (1:1) were also
118 analysed. Infra-red spectra were recorded on a FTIR 100 series Perkin-Elmer spectrometer
119 fitted with a deuterated triglycine sulphate (DTGS) detector using the Universal attenuated
120 total reflectance (ATR) mode. Spectra were recorded at ambient temperature (22 ± 2 °C) on

121 solid samples at a resolution of 4 cm^{-1} and a scan number of 32 over the range of 4000–650
122 cm^{-1} with air as background. FTIR spectra of freeze dried Lf samples were similar to that of
123 commercial as received samples (data not shown).

124 The structural conformation of Lf in the Lf-alginate solutions was studied by CD
125 spectroscopy. The spectra of Lf, alginate and Lf-alginate mixtures (1:1) in aqueous solution
126 were recorded in aqueous solution with Millipore water as the background in the wavelength
127 region 250–350 nm using a Jasco J-710 spectrometer with a J-700 Spectra manager software.
128 Lf and alginate samples were diluted to 0.25 % while Lf-alginate mixtures were diluted to
129 0.50 % for analysis. The measurements were made at ambient temperature ($22 \pm 2\text{ }^\circ\text{C}$) and
130 the ellipticities were expressed as Milli degrees.

131 Surface charge properties of the Lf, alginate and Lf-alginate mixtures were measured using
132 NanoS Zetasizer based on electrophoretic mobility of the particles. The solutions used for the
133 measurements were acetate buffer (pH 4 and 5) and bis-tris buffer (pH 6 and 7) all with a
134 final ionic concentration of 1 mM potassium chloride as well as water resulting in natural pH
135 (the pH which is achieved upon dissolution of the protein). Solutions of Lf (apo-, native- and
136 holo-) and sodium alginate were prepared in appropriate media (1% w/w). Lf was dissolved
137 at constant stirring for 2 h at room temperature using a magnetic stirrer. Sodium alginate was
138 dissolved using high shear homogeniser (IKA® RW 20 digital, USA) at 600 rpm for 30 min.
139 The alginate solution was then heated in a water bath at $40\text{ }^\circ\text{C}$ for 90 min to remove any
140 trapped air bubbles. The Lf and alginate solutions were mixed in a ratio of 1:1 using the high
141 shear homogeniser (~500 rpm for 5 min). The mixture was allowed to stand at room
142 temperature for 1 h. The zeta-potential was measured after diluting the mixtures 50 times.

143 Lf and alginate mixtures were examined using 12% polyacrylamide precast continuous gels
144 (Mini-PROTEAN® TGXTM Precast Gels, BIO-RAD, Gladesville, Australia) under non-

145 denaturing (native) conditions in a Mini-PROTEAN tetra cell system. The samples of Lf and
146 Lf-alginate mixtures (2 % w/w) were diluted in Millipore water to achieve 1 mg/mL of
147 protein (Lf) content. The loading buffer contained 70 mM Tris-Cl (pH 6.8), 31 % glycerol
148 and 0.01 % bromophenol blue as the dye. The samples were diluted with the loading buffer in
149 the ratio of 1:2 prior to loading in the precast gel. Diluted samples (5 μ L) were loaded into
150 the wells of the precast gel and electrophoresis was carried out at 200 V. The gels were fixed
151 for 5 min, stained with Coomassie brilliant blue R-250 solution (34 % methanol) and finally
152 destained. The gel was scanned using Gel Densitometer (GS-800 Calibrated Densitometer,
153 UMAX Technologies, Model UTA – 2100XL, Taiwan) and analysed with Quantity One®
154 software operating in Microsoft Windows® computer system. To evaluate the effect of
155 holding time on complexation between alginate and Lf in aqueous solution, Native-PAGE
156 was run for Lf-alginate mixtures (1:1) on different days; day 0 (immediately after mixing),
157 day 1 and day 7. Apart from day 0, the mixtures were kept at 5 °C. In addition, Native-PAGE
158 gels with alginate and Lf-alginate mixtures in equal mixing ratio (1:1) were stained using
159 Periodic Acid Schiff (PAS) technique used for carbohydrate staining (Dubray & Bezar,
160 1982). The gel was fixed in fixative solution for 5 min followed by 1% periodic acid solution
161 dip for 10 min. It was then rinsed with Millipore water twice for an interval of 10 min each
162 and was dipped in Schiff's reagent for 10 min. Finally the gel was allowed to remain in
163 Millipore water overnight and scanned as described above.

164 The apparent viscosity of the Lf, alginate and Lf-alginate mixtures at natural pH (unaltered)
165 was measured by a Discovery Hybrid Rheometer (DHR-1; TA Instruments, USA) using
166 TRIOS software at 20 °C under the shear rate of 25 s⁻¹. A 40 mm, parallel plate, peltier plate
167 steel geometry was used with a gap of 100 μ m. Stock solutions of alginate (2 % w/w) and
168 apo-, native- and holo-Lf as well as Lf-50 (Lf having 50% iron saturation level) (2 % w/w)
169 were prepared in Millipore water and mixed at different ratios to achieve total Lf content of

170 25, 50, 60 and 75 % of the final 2 % total solid content in the mixtures. As controls, 2 %
171 alginate stock solution was diluted with Millipore water to achieve total solid content of 0.5,
172 0.8, 1.0 and 1.5 % (w/w). Furthermore, Lf-alginate mixtures with similar mixing ratios but
173 with different solid concentrations were prepared. Mixing was done using a high shear
174 homogeniser (~500 rpm for 5 min) and the solutions were left at room temperature overnight
175 before the measurement. In order to evaluate the contribution of addition of Lf to the
176 viscosity of the mixture, the increase in viscosity due to Lf addition to the alginate solution
177 was calculated as follows:

$$178 \quad \text{Contribution of Lf to viscosity} = \frac{\text{Viscosity (Mixture)} - \text{Viscosity (Alginate)}}{\text{Viscosity (Mixture)}} \times 100\% \quad (1)$$

179 -ie. from the viscosity of 2% mixture containing x % alginate, viscosity of x % alginate was
180 subtracted.

181 The thermal properties of different forms of Lf in the presence of alginate in aqueous solution
182 were studied by Differential Scanning Calorimetry (DSC1 STAR^e System, METTLER
183 TOLEDO, Schwerzenbach, Switzerland) according to the method described by Bokkhim,
184 Bansal, Grøndahl and Bhandari (2013). The Lf-alginate mixtures (2 % w/w) at 1:1 mixing
185 ratio were prepared in Millipore water, allowed to stand at room temperature (22 ± 2 °C)
186 overnight and freeze dried. The freeze dried Lf-alginate samples were rehydrated in Millipore
187 water to achieve 10 % solutions. 20 µL of rehydrated Lf-alginate mixtures were used for
188 analysis. The temperature of maximum heat absorption (T_{\max}) and the enthalpy change of
189 denaturation (ΔH_{cal}) were determined from the transition peak using STAR^e Excellence
190 Software (METTLER TOLEDO). It was not possible to prepare 10% Lf-alginate mixture by
191 simply dissolving and mixing, thus freeze drying of the Lf-alginate mixture was done.

192 **Statistical analysis**

193 Zeta-potential values and thermal properties are presented as mean \pm SD of triplicate
194 experiments. MiniTab 16 software was used to analyse the significance of differences
195 between the values (where applicable) using Analysis of Variance (ANOVA) with Tukey's
196 HSD post hoc test at family error rate 5 at 95% confidence level.

197 **Results and Discussion**

198 This study investigated the properties of Lf-alginate mixtures prepared from different forms
199 of Lf and at different mixing ratios with a constant final solid content of 2% at pH values of
200 4–7. This pH range was chosen based on the fact that Lf is unstable below pH 4.0 (Abdallah
201 & El Hage Chahine, 2000), that the pKa of alginate is 3.4–3.7 and the pI of Lf is 7.8–9.5.
202 Furthermore, this is the pH range most commonly encountered in food products. After
203 combining the Lf and the alginate solutions, the mixtures were held at 4 ± 2 °C overnight to
204 ensure equilibrium had been attained. Neither precipitation nor gelling was visible in the
205 mixtures. The formation of soluble complexes is attributed to the mixing ratios studied for
206 which the net charge of alginate far surpassed the charge of Lf. Relatively stable colloidal
207 dispersions of a native-Lf-alginate system at pH 3–10 has previously been reported for
208 aggregated Lf particles (Peinado et al., 2010).

209 **Chemical Characterisation**

210 FTIR spectra of alginate, different forms of Lf and their respective freeze dried composite Lf-
211 alginate mixtures (1:1) were analysed in the wavelength region of 1200–1750 cm^{-1} . In
212 addition, physical mixtures (e.g. dry-mixed powders) of alginate and Lf (1:1) were run as
213 control samples. The wavelength region chosen includes the amide I (1600–1690 cm^{-1}), II
214 (1480–1575 cm^{-1}) and III (1229–1301 cm^{-1}) bands of proteins (Kong & Yu, 2007) as well as
215 the antisymmetric stretch (1595–1597 cm^{-1}) and symmetric stretch (1407–1412 cm^{-1}) of the

216 carboxylate groups of alginate (Lawrie et al. 2007). Figure 1 (A, B & C) show the spectral
217 data obtained. The amide I and amide II bands observed at $1637\text{--}8\text{ cm}^{-1}$ and around 1520
218 cm^{-1} , respectively, for all three forms of Lf in the dry state are different to those reported for
219 human-Lf in solution (1647 and 1577 , respectively) (Hadden, Bloemendal, Haris, Srai &
220 Chapman, 1994), however, fall within the expected regions for amide bands.

221 For apo- and native-Lf it was possible to obtain representative spectra of the physical mixture
222 (dry mixed powders) of Lf and alginate (1:1) as control samples, however, such a sample
223 could not be obtained for holo-Lf as the consistency of the powder prevented proper mixing
224 in the dry state. The physical mixtures show the addition spectra of the two macromolecules
225 in which no intermolecular interactions occur. It can be seen in Figure 1 (A & B) that the
226 major bands and shoulders in these samples are very similar to that of the two pure
227 macromolecules but with an apparent shift in the amide I band to lower wavenumbers of
228 around $7\text{--}8\text{ cm}^{-1}$ which is attributed to the underlying antisymmetric stretching of the
229 carboxylate group of alginate. Importantly, in the freeze-dried samples prepared from mixing
230 Lf with alginate (1:1) in solution and subsequent drying intermolecular interactions can
231 occur, and here the amide I band is found in a similar position to the physical mixture
232 indicating that there is no change in the secondary structure of the protein. Likewise, the
233 apparent shift in the amide II band to higher wavenumbers by $17\text{--}10\text{ cm}^{-1}$ is attributed to an
234 additive effect as the same trend was noticed for the physical mixtures. The position of the
235 amide III band was not affected by the addition of alginate in the mixture.

236 The antisymmetric stretch of alginate showed a shoulder in the physical mixture at a similar
237 position as pure alginate (e.g. at 1595 cm^{-1}). However, in the freeze dried mixture a shift in
238 this band towards higher wavenumber by $8\text{--}9\text{ cm}^{-1}$ was evident (Figure 1). Furthermore, the
239 separation (Δ) between the antisymmetric and symmetric stretching vibrations (Lawrie et al.

240 2007) change from 188 cm^{-1} in alginate to $198\text{--}200\text{ cm}^{-1}$ in the freeze-dried samples and this
241 is attributed to the carboxylate group of alginate interacting with Lf, most likely with the
242 positively charged amino acid side chains. The spectral features for such amino acid side
243 chains are unfortunately not well resolved but overlap with the amide vibrational modes. In a
244 similar manner to these findings, different changes in the FTIR spectra of freeze-dried and
245 physical mixtures have also been reported by Souillac, Middaugh and Rytting (2002) in a
246 protein/carbohydrate mixture. Zhao et al. (2009) displayed in their work on bovine serum
247 albumin added to sodium alginate in solution some shifts in the FTIR bands, however, in
248 their work, the spectra were not compared to a simple addition spectrum of the two
249 macromolecules. Overall, in agreement with the general observation that proteins
250 electrostatically binds mostly with the carboxyl groups of the polysaccharides (Tolstoguzov,
251 1991) the FTIR spectra indicate the presence of intermolecular interactions between Lf and
252 alginate in the freeze-dried mixture involving the carboxylate groups of alginate, however,
253 these interactions do not cause a change the secondary structure of the protein.

254 Figures 1A, 1B and 1C

255 CD spectroscopy is a well-established tool for the assessment of changes to the tertiary
256 structure of proteins-polyelectrolyte complexes (Kayitmazer, Seeman, Minsky, Dubin, & Xu,
257 2013). The CD spectra of alginate, different forms of Lf and their respective mixtures (1:1) in
258 aqueous solution in wavelength region of $250\text{--}350\text{ nm}$ are shown in Figure 2. This
259 wavelength region was chosen as it was where the ellipticity values of alginate in solution lie
260 in the vicinity of zero and therefore allows evaluation of the Lf tertiary structure. All spectra
261 showed the characteristic bands of Lf in the $250\text{--}350\text{ nm}$ region; a negative band centered at
262 $270\text{--}272\text{ nm}$, a band at $291\text{--}292\text{ nm}$ and one at $296\text{--}298\text{ nm}$ (Bokkhim et al., 2013). Within
263 experimental error there was very good agreement between the spectra of each of the forms

264 of Lf and their respective mixtures with alginate and no significant change in the maximum
265 wavelength or ellipticity values was observed. This demonstrates that despite the
266 intermolecular interactions that occur between the oppositely charged Lf and alginate in
267 aqueous solution, all forms of Lf retained their original tertiary structures. This result is in
268 agreement with previous findings that oxidised sodium alginate does not induce a
269 conformational change to BSA (Gao, Liu, Chen, & Chen, 2011).

270 Figure 2

271 **Physicochemical Characterisation**

272 The zeta-potential of native-Lf-alginate mixtures at different mixing ratios in the pH range
273 4.0– 7.0 was studied. The Native-Lf mixture displays a positive zeta-potential in this pH
274 range in agreement with its *pI* value and it was found that the zeta-potential was significantly
275 higher at pH 4 as seen in Figure 3A. In the absence of Lf, alginate displayed similar zeta-
276 potential values in the pH range studied (Fig. 3A). With the addition of Lf, the negative
277 charge decreased significantly (the zeta-potential values of the mixtures were significantly
278 different ($P < 0.05$) to that of the alginate solution at all pH values studied) and the decrease
279 was larger at lower pH (Fig. 3A). This correlates with the significantly more positive charge
280 of Lf at pH 4. In addition, it was noted that the higher the amount of Lf in the mixture, the
281 larger was the numerical decrease in the zeta-potential value (Fig. 3B). A similar trend was
282 noted when Lf was added to negatively charged β -lactoglobulin-stabilized emulsions (Ye &
283 Singh, 2007) and is in agreement with formation of electrostatic interactions between the two
284 macromolecules (Ye, 2008). Since the largest decrease in zeta-potential was observed for the
285 mixture with the alginate:Lf ratio of 1:1 (Fig. 3B) this mixing ratio was chosen for further
286 experiments. Furthermore, the zeta-potential values of the native-Lf-alginate mixtures were
287 not significantly different at pH 4 and 5 or at pH 6 and 7. However, the zeta-potential values

288 of the mixtures at pH 4 or 5 were significantly different ($P < 0.05$) from that at pH 6 or 7
289 (Fig. 3 A). Based on this, the three forms of Lf were studied at pH 4 and 7.

290 The zeta-potential of the three forms of Lf, alginate and Lf-alginate mixtures at pH 4 and 7
291 are presented in Figure 3C. The zeta-potential values for all three forms of Lf at both pH 4
292 and 7 were positive and the value for apo-Lf was significantly lower than that of native- and
293 holo-Lf at both pH values in agreement with that previously reported (Bokkhim et al., 2013).
294 In addition, zeta-potential values of all Lf solutions at pH 7 were much lower than at pH 4 as
295 noted above for native-Lf. It was found that the Lf-alginate mixtures generated significantly
296 different ($P < 0.05$) zeta-potential values than that of alginate at both pH values. The
297 differences in zeta-potential for the different forms of Lf in mixtures were insignificant at
298 both pH 4 and 7. It can be inferred that the negative charges of alginate were partly
299 compensated by the addition of positively charged Lf. Thus, as can be seen from Figure 3C, a
300 more positive zeta-potential of Lf at pH 4 resulted in higher charge compensation when
301 added to negatively charged alginate solution leading to a significant decrease in the zeta-
302 potential. At pH 7, which is near the pI of Lf, the protein had a lower positive charge thus
303 leading to lower charge compensation. The results obtained are in agreement with the
304 formation of electrostatic interaction between all forms of Lf and alginate at both pH 4 and 7.
305 The overall negative charge of the complexes similar to that of the polyelectrolyte alginate
306 indicates that the outer layer of the complex is dominated by the polyelectrolyte (Peinado et
307 al., 2010).

308 Figures 3A, 3B, 3C and 3D

309 The surface charge properties of the three forms of Lf, alginate and Lf-alginate mixtures at
310 natural (unaltered) pH are presented in Figure 3D. From previous studies it has been found
311 that pH of 1 % (w/w) natural apo-, native- and holo-Lf solutions are 5.7, 5.4 and 6.2,

312 respectively (Bokkhim, et al., 2013). It was found that the zeta-potential of apo-Lf was
313 significantly lower (5.3 ± 0.1 eV) than native- and holo-Lf (18 ± 1 eV and 22.3 ± 0.4 eV,
314 respectively) under these conditions (Fig. 3D). Furthermore, it was found that the zeta-
315 potential values of Lf-alginate mixtures at natural pH in different mixing ratios (alginate:Lf =
316 1:1 and 1:1.5) were not significantly different from each other, but were significantly
317 different from that of alginate at both mixing ratios (Fig. 3D). This lack of a discernable
318 change in the zeta-potential values with the additional Lf in the mixture could indicate that a
319 point of saturation of alginate has been reached or that the difference is too small to detect. In
320 the following sections the mixtures were studied under natural pH conditions as this is most
321 relevant to Lf encapsulation in alginate for its development as a pharmaceutical or food
322 component.

323 **Evaluation of Relative Binding Affinity of Different Forms of Lf**

324 Evaluation of protein-polyelectrolyte interactions has traditionally used capillary
325 electrophoresis and size exclusion chromatography (Kayitmazer et al., 2013). More recently,
326 so-called gel retardation assays employing agarose gels have been used to evaluate
327 complexation between DNA and chitosan (Masotti et al., 2007) and complexation between
328 silk-polylysine block copolymers and plasmid DNA (Numata, Subramanian, Currie, &
329 Kaplan, 2009) while heparin displacement assays employing native polyacrylamide gel
330 electrophoresis has been used to evaluate complex stability for complexes between siRNA
331 and PEI polyelectrolytes (Hobel et al., 2011). Common to these techniques is the ability to
332 evaluate relative amounts of bound and unbound protein/polynucleotide. In the current study,
333 Native-PAGE gel electrophoresis was explored as a means to evaluate to which extent
334 alginate is capable of binding the different forms of Lf. The choice of native conditions for
335 the gel electrophoresis experiment was based on the protein tertiary structure being retained

336 under these conditions. In order to test this concept a gel was run with native-Lf at a constant
337 amount in all lanes but in different mixing ratios with alginate and the result of a Coomassie
338 blue stained gel (protein stain) is displayed in Figure 4A. It can be seen, that in all samples a
339 protein band is appearing at the same position as the positive control (native-Lf in the
340 absence of alginate, lane 1). Furthermore, in lanes containing alginate, varying amounts of Lf
341 has remained on the top of the gel and the amount migrated (values indicated on the gel)
342 increases with decreasing amount of alginate (from lane 2 to 10). This result is interpreted in
343 terms of the Lf associated with alginate being prevented from migrating in the
344 polyacrylamide gel (ie. it is being retarded) and remain at the top of the gel while un-bound
345 Lf has migrated. This clearly demonstrates the validity in using native-PAGE to evaluate
346 (relative) binding of Lf to alginate. It should be noted, that over the mixing ratio range
347 studied there is a 100 fold difference in the molar ratio of alginate to Lf and this is not linear
348 which explains the non-linear trend in the amount of migrated Lf with mixing ratio.
349 Furthermore, this result agrees with the lack of a discernable change in the zeta-potential
350 values for the two mixing ratios evaluated in Figure 3D.

351 Figures 4A and 4B

352 Subsequently, Native-PAGE gel electrophoresis was used to evaluate relative binding affinity
353 of the different forms of Lf to alginate. The result shown in Figure 4B was obtained at a
354 constant mixing ratio of 1:1 and a constant amount of Lf in all lanes and the protein stained
355 using Coomassie blue. It can be seen that all forms of Lf appear at the same position as the
356 respective positive control samples (lanes 1, 5, 9). Furthermore, the effect of holding time
357 over 7 days was evaluated. Within the experimental error, there was no significant difference
358 in the amount of Lf migrating with different loading time for either apo-Lf (lanes 2–4),
359 native-Lf (lanes 6–8) or holo-Lf (lanes 10–12). Therefore, the amount of the different forms

360 of Lf bound to alginate was evaluated from the average values from the three time points and
361 found to be 76% for apo-Lf, 60% for native-Lf and 60% for holo-Lf. Repeat experiments
362 (data not shown) consistently showed that a larger amount of protein was retained in the apo-
363 Lf complex compared to the other proteins. A separate gel was run and stained with PAS
364 (polysaccharide stain, Supplementary Figure S1). This experiment showed that for all
365 proteins a similar amount of alginate was retained for the complexes relative to the pure
366 alginate sample. It can thus be concluded that that alginate displays higher binding capacity
367 (larger number of protein molecules per alginate polymer) for apo-Lf than for the other forms
368 of Lf. This result correlates with the surface charge properties of the different forms of Lf at
369 natural pH. Thus, apo-Lf is close to its isoelectric point while the two other forms of Lf have
370 similar positive surface charge (Fig. 3D). While one study found that proteins with higher
371 (and opposite) charge resulted in more binding events with polyelectrolytes (Vinayahan,
372 Williams, & Phillips, 2010), another study has shown, that not only the overall charge but
373 also the charge distribution of proteins affect their interactions with polyelectrolytes (Xu,
374 Mazzawi, Chen, Sun, & Dubin, 2011). In the current study it appears that the higher capacity
375 for alginate to bind apo-Lf compared to native- and holo-Lf is related to fewer intermolecular
376 interactions between alginate and apo-Lf. Considering that the strength of interaction between
377 oppositely charged biopolymers is enhanced when the net charges of the biopolymers are
378 increased (Ye, 2008), this in turn leads to the prediction that weaker interactions exist
379 between alginate and apo-Lf than the other forms of Lf.

380 **Properties of Mixtures Resulting from Intermolecular Interactions**

381 The polysaccharide alginate is expected to affect the viscosity more than the protein Lf
382 (Schmitt, Sanchez, Desorby-Banon, & Hardy, 1998). However, electrostatic interactions
383 between Lf and alginate can affect the apparent viscosity of their mixtures. It should be noted

384 that the change in viscosity might not always result from an electrostatic interaction but also
385 from other intermolecular interactions and hydration properties of the molecules involved.
386 Mixing of polymers can influence the hydration property of a polymer in the mixture and
387 there can be a synergistic (compatibility) or antagonistic (non-compatibility) effect
388 (Tolstoguzov, 1991). When native-Lf (2 % w/w) having very low viscosity (~2 mPa s) was
389 added to an alginate (2 % w/w) solution of high viscosity (~1300 mPa s) at an equal ratio
390 (1:1) (resulting in 1% alginate), the apparent viscosity of the mixture was found to be much
391 higher (~1000 mPa s) than that of 1 % alginate solution alone (~150 mPa s) but lower than
392 that of a 2 % alginate solution. This clearly showed that the viscosity of the mixture was not
393 solely due to alginate and that Lf synergistically contributed to the increase in viscosity. If the
394 result of mixing alginate and Lf had been an additive effect, the viscosity would have
395 decreased to a value similar to that of the 1 % alginate solution as the viscosity of the Lf
396 solution is significantly lower than that of the alginate solution at the same concentrations.
397 The results clearly indicated that intermolecular interactions between Lf and alginate have an
398 effect on the viscosity of their mixtures.

399 The effect of iron saturation levels on the viscosity change in mixtures with constant total
400 solid content of 2 % (w/w) was studied. From Figure 5A, it can be seen that with the increase
401 in apo-Lf, Lf-50 and holo-Lf content in the mixture from 25 to 75 % (e.g. mixing ratios of 3:1
402 to 1:3), the viscosity of the mixture decreased. However, the contribution of Lf on viscosity
403 increments as calculated by equation 1 increased for the same series of mixtures (Fig. 5B).
404 For native-Lf, on the other hand, the viscosity of the mixture increased along with its
405 contribution to viscosity increment. Comparing the native-Lf, Lf-50 and holo-Lf at any Lf
406 content, it can be seen that with an increasing level of iron saturation of Lf, the viscosity
407 increment decreased. Considering that the iron ions are buried within the interdomains of the
408 lobes of the protein (Brisson et al., 2007) they are unlikely to affect the intermolecular

409 interactions. However, upon iron binding a change in tertiary structure of Lf is observed
410 (Bokkhim, Tran, Bansal, Grøndahl, & Bhandari, 2014; Shimazaki, Kawano, & Yoo, 1991)
411 which appears to affect the strength of intermolecular interactions with alginate and is likely
412 due to the availability of exposed functional groups on Lf changing as a consequence of the
413 change in tertiary structure. Considering that apo-Lf has the lowest iron saturation it would be
414 predicted to have the highest impact on the viscosity increment, however, this was not
415 observed. This can be related to these experiments being done at the natural pH of the Lf, and
416 the fact that apo-Lf has a significantly lower zeta-potential compared to native- and holo-Lf
417 under these conditions (Fig. 3D) thus decreasing electrostatic interaction with anionic
418 alginate as concluded above. The native-Lf showed the maximum increase in viscosity of the
419 mixture at any Lf content level. The amount of native-Lf bound to alginate for mixtures
420 containing 50 % or more native-Lf remain relatively constant (Figure 4A), yet, a large effect
421 on viscosity is seen between 50, 60 and 75 % Lf content. One explanation for this observation
422 is that as the amount of alginate decreases relative to native-Lf, there will be less alginate
423 available per Lf molecule which gives rise to network formation although not to an extent of
424 visible gelling. This would cause the viscosity to increase with increasing amount of native-
425 Lf in the mixture. The native-Lf is unique in displaying this property and this is contributed
426 to a combination of optimal tertiary structure as well as optimal surface charge properties.

427 Figures 5A and 5B

428 The changes in thermal properties of Lf in the Lf-alginate mixtures in aqueous solution at
429 natural pH were studied by DSC. The temperature of maximum heat absorption (T_{\max}), also
430 known as the denaturation peak, and the enthalpy change of denaturation (ΔH_{cal}) were
431 derived from the transition peak obtained from the DSC thermograms and the values are
432 presented in Table 1. The denaturation peaks of apo-Lf and the second peak (mono- or di-

433 ferric saturated) of the native-Lf (Bokkhim et al., 2014) in the mixtures were not significantly
434 different from their respective Lf samples. However, the denaturation peaks of the first
435 (main) peak (iron free) of native-Lf and the peak of holo-Lf in the mixtures shifted
436 significantly towards higher temperature as compared to their respective Lf samples. Though
437 apo-Lf and the first peak (iron free) of native-Lf both are devoid of iron and similar in
438 composition, the difference in their behaviour in the mixtures can be related to differences in
439 the strength of intermolecular interactions with alginate as a result of their surface charge
440 properties. The significant increase in the denaturation temperatures for native- and holo-Lf
441 in their alginate mixtures is attributed to a larger number of electrostatic interactions as
442 inferred from the PAGE gel electrophoresis data. The reason for the second peak of native-Lf
443 not showing a significant increase in denaturation temperature can be attributed to the small
444 amount of iron saturated Lf (mono- or di-ferric) present in the native-Lf (13 %). In agreement
445 with the current study, improved heat stability of Lf in the presence of negatively charged
446 soluble soybean polysaccharide has been reported (Uneo, Ueda, Morita, Kakehi, &
447 Kobayashi, 2012). Tolstoguzov (1991) pointed out that in a protein-polysaccharide mixture,
448 increasing the amount of bound protein in the mixture gives rise to an increase in the
449 denaturation temperature of the protein as compared to free proteins. Considering that only
450 60 % of native- and holo-Lf is bound to alginate at the mixing ratio studied (1:1) and that this
451 can be increased upon changing the mixing ratio (based on PAGE gel electrophoresis results),
452 it is clear that alginate offers great opportunity for improving the thermal stability of Lf.

453 The enthalpy change of denaturation (ΔH_{cal}) for the main denaturation peak for all the
454 mixtures significantly decreased as compared to their respective Lf samples. Though a higher
455 temperature was needed to denature Lf in the mixtures attributed to intermolecular
456 interactions, less heat energy was required to cause denaturation once the temperature of
457 denaturation had been reached. Previous studies reported in the literature have made disparate

458 observations with regards to the effect of polyelectrolytes on protein stability. A study of
459 mixtures of polysulfoanions and glyceraldehyde-3-phosphate dehydrogenase (GADPH)
460 found that these polyelectrolytes cause a decrease in denaturation temperature and that
461 polysaccharide-based polyelectrolytes had the least of an effect (Stogov, Izumrudov &
462 Muronetz, 2010). Likewise, synthetic anionic polyelectrolytes when complexed with
463 lysozyme, chymotrypsinogen and GADPH were found to significantly reduce the thermal
464 stability of the protein (Inivova, Izumrudov, Muronetz, Galaev & Mattiasson, 2003). In
465 contrast, Burova et al. (2002) has made similar observations to the current study. They
466 reported a lowering of the denaturation enthalpy for complex of soybean tripsin (Kunitz)
467 inhibitor (STI) and dextran sulfate at pH 3 and an increase in denaturation temperature of STI
468 when complexed with pectin having low degree of esterification.

469 Overall, these and the current study highlight the importance of evaluating the thermal
470 stability of protein/polyelectrolyte complexes before proceeding for technological
471 application. Furthermore, the current study have shown that while alginate does not enhance
472 the thermal stability of Lf, it does lead to a higher denaturation temperature which is an
473 important finding for the application of Lf-alginate mixtures in food products.

474 Table 1

475 **Conclusion**

476 The results of this study have demonstrated that the anionic polysaccharide alginate has the
477 potential to be a successful carrier material for different forms of Lf since the protein is
478 conformational stable in its mixtures with alginate. A number of the experiments probed the
479 intermolecular interactions between alginate and the different forms of Lf. Specifically; the
480 zeta-potential data was consistent with charge compensation of the protein by alginate with
481 the overall complex carrying a negative charge in the pH range of 4 to 7. It was shown from

482 the FTIR spectra that the COO⁻ moieties of alginate are involved in the intermolecular
483 interactions and the viscosity of the mixtures furthermore gave strong indications of
484 intermolecular interactions. In addition, it was found in this study that the form of Lf has a
485 significant effect on both the binding affinity (from PAGE gel electrophoresis) and strength
486 of interactions (from viscosity and DSC) in these complexes. This knowledge will be of great
487 value when fabricating alginate-based delivery systems for Lf. Further work is being carried
488 out on the *in-vitro* release of lactoferrin from Lf-alginate encapsulate mixture.

489 **Acknowledgements**

490 The authors thank Dr Chandhi Goonasekera, School of Chemistry and Molecular
491 Biosciences, The University of Queensland for her assistance in determining the molecular
492 mass of the alginate sample used in this study.

493

494

495

496

497

498

499

500

501

502

503

504

505 **References**

- 506 Abdallah, F. B., & El Hage Chahine, J.-M. (2000). Transferrins: iron release from lactoferrin.
507 *Journal of Molecular Biology*, 303(2), 255-266.
- 508 Abe, H., Saito, H., Miyakawa, H., Tamura, Y., Shimamura, S., Nagao, E., & Tomita, M.
509 (1991). Heat stability of bovine lactoferrin at acidic pH. *Journal of Dairy Science*, 74(1), 65-
510 71.
- 511 Baker, E. N. (2005). Lactoferrin: A multi-tasking protein par excellence. *Cellular and*
512 *Molecular Life Sciences*, 62(22), 2529-2530.
- 513 Bengoechea, C., Jones, O. G., Gerrero, A., & McClements, D. J. (2011). Formation and
514 characterization of lactoferrin/pectin electrostatic complexes: Impact of composition, pH and
515 thermal treatment. *Food Hydrocolloids*, 25(5), 1227-1232.
- 516 Bengoechea, C., Peinado, I., & McClements, D. J. (2011). Formation of protein nanoparticles
517 by controlled heat treatment of lactoferrin: Factors affecting particle characteristics. *Food*
518 *Hydrocolloids*, 25(5), 1354-1360.
- 519 Benichou, A., Aserin, A., & Garti, N. (2002). Protein-polysaccharide interactions for
520 stabilization of food emulsions. *Journal of Dispersion Science and Technology*, 23(1-3), 93-
521 123.
- 522 Bokkhim, H., Bansal, N., Grøndahl, L., & Bhandari, B. (2013). Physico-chemical properties
523 of different forms of bovine lactoferrin. *Food Chemistry*, 141, 3007-3013.
- 524 Bokkhim, H., Tran, T. N. H., Bansal, N., Grøndahl, L., & Bhandari, B. (2014). Evaluation of
525 different methods for determination of the iron saturation level in bovine lactoferrin. *Food*
526 *Chemistry*, 152, 121-127.
- 527 Brisson, G., Britten, M., & Pouliot, Y. (2007). Heat-induced aggregation of bovine lactoferrin
528 at neutral pH: Effect of iron saturation. *International Dairy Journal*, 17(6), 617-624.
- 529 Burova, T. V., Varfolomeeva, E. P., Grinberg, V. Y., Haertlé, T., & Tolstoguzov, V. B.
530 (2002). Effect of polysaccharides on the stability and renaturation of soybean trypsin (Kunitz)
531 inhibitor. *Macromolecular Bioscience*, 2(6), 286-292.

- 532 Conneely, O. M., & Ward, P. P. (2004). Lactoferrin: Role in iron homeostasis and host
533 defense against microbial infection. *BioMetals*, *17*(3), 203-208.
- 534 Draget, K. I. (2009). Alginates. In Phillips, G. O. & Williams, P. A. (Eds.), *Handbook of*
535 *Hydrocolloids* (2nd ed.). (pp. 807-828). Cambridge, UK: Woodhead Publishing Limited.
- 536 Dubray, G., & Bezard, G. (1982). A highly sensitive periodic acid-silver stain for 1,2-diol
537 groups of glycoproteins and polysaccharides in polyacrylamide gels. *Analytical Biochemistry*,
538 *119* (2), 325-329.
- 539 Eriksen, E. K., Holm, H., Jensen, E., Aaboe, R., Devold, T. G., Jacobsen, M., & Vegarud,
540 G. E. (2010). Different digestion of caprine whey proteins by human and porcine
541 gastrointestinal enzymes. *British Journal of Nutrition*, *104*, 374-381.
- 542 Gao, C., Liu, M., Chen, J., & Chen, C. (2011). Interactions between bovine serum albumin
543 and oxidized sodium alginate in solution. *Journal of Biomaterials Science, Polymer Edition*,
544 *22* (12), 1639-1650.
- 545 Gombotz, W. R., & Wee, S. (1998). Protein release from alginate matrices. *Advanced Drug*
546 *Delivery Reviews*, *31*(3), 267-285.
- 547 Gu, F., Amsden, B., & Neufeld, R. (2004). Sustained delivery of vascular endothelial growth
548 factor with alginate beads. *Journal of Controlled Release*, *96*(3), 463-472.
- 549 Guo, P., Pan, Y., Rowney, M., & Hobman, P. (2007). Biological properties of lactoferrin: an
550 overview. *Australian journal of dairy technology*, *62* (1), 31-42.
- 551 Ivinova, O. N., Izumrudov, V. A., Muronetz, V. I., Galaev, I. Y., & Mattiasson, B. (2003).
552 Influence of complexing polyanions on the thermostability of basic proteins. *Macromolecular*
553 *Bioscience*, *3*(3-4), 210-215.
- 554 Kayitmazer, A. B., Seeman, D., Minsky, B. B., Dubin, P. L., & Xu, Y. (2013). Protein-
555 polyelectrolyte interactions. *Soft Matter*, *9* (9), 2553-2583.
- 556 Kong, J., & Yu, S. (2007). Fourier transform infrared spectroscopic analysis of protein
557 secondary structures. *Acta Biochimica et Biophysica Sinica*, *39*(8), 549-559.
- 558 Hadden, J. M., Bloemendal, M., Haris, P. I., Srail, S. K. S., & Chapman, D. (1994). Fourier
559 transform infrared spectroscopy and differential scanning calorimetry of transferrins: human

- 560 serum transferrin, rabbit serum transferrin and human lactoferrin. *Biochimica et Biophysica*
561 *Acta*, 1205, 59-67.
- 562 Höbel, S., Loos, A., Appelhans, D., Schwarz, S., Seidel, J., Voit, B., & Aigner, A. (2011).
563 Maltose- and maltotriose-modified, hyperbranched poly(ethylene imine)s (OM-PEIs):
564 Physicochemical and biological properties of DNA and siRNA complexes. *Journal of*
565 *Controlled Release*, 149 (2), 146-158.
- 566 Lawrie, G., Keen, I., Chandler-Temple, A., Drew, B., Rintoul, L., Fredericks, P., & Grøndahl,
567 L. (2007). Interactions between alginate and chitosan biopolymers characterised using FTIR
568 and XPS. *Biomacromolecules*, 8 (8), 2533-2541.
- 569 Masotti, A., Moretti, F., Mancini, F., Russo, G., Di Lauro, N., Checchia, P., Marianecchi, C.,
570 Carafa, M., Santucci, E., & Ortaggi, G. (2007). Physicochemical and biological study of
571 selected hydrophobic polyethylenimine-based polycationic liposomes and their complexes
572 with DNA. *Bioorganic & Medicinal Chemistry*, 15 (3), 1504-1515.
- 573 McClements, D. J. (2006). Non-covalent interactions between proteins and polysaccharides.
574 *Biotechnology Advances*, 24(6), 621-625.
- 575 Moore, S. A., Anderson, B. F., Groom, C. R., Haridas, M., & Baker, E. N. (1997). Three-
576 dimensional structure of diferric bovine lactoferrin at 2.8 Å resolution. *Journal of Molecular*
577 *Biology*, 274 (2), 222-236.
- 578 Naidu, A. S. (2006). Treatment of case-ready food products with immobilized lactoferrin
579 (IM-LF) and the products so produced. *U.S. Patent No. 7,074,759 B2*. Alexandria, VA: US
580 Patent and Trademark Office.
- 581 Numata, K., Subramanian, B., Currie, H. A., & Kaplan, D. L. (2009). Bioengineered silk
582 protein-based gene delivery systems. *Biomaterials*, 30 (29), 5775-5784.
- 583 Onishi, H. (2011). Lactoferrin delivery systems: approaches for its more effective use. *Expert*
584 *Opinion on Drug Delivery*, 8(11), 1469-1479.
- 585 Peinado, I., Lesmes, U., Andrés, A., & McClements, J. D. (2010). Fabrication and
586 morphological characterization of biopolymer particles formed by electrostatic complexation
587 of heat treated lactoferrin and anionic polysaccharides. *Langmuir*, 26(12), 9827-9834.

- 588 Schmitt, C., & Turgeon, S. L. (2011), Protein/polysaccharide complexes and coacervates in
589 food systems. *Advances in Colloid and Interface Science*, 167, 63-70.
- 590 Schmitt, C., Sanchez, C., Desorby-Banon, S., & Hardy, J. (1998). Structure and
591 technofunctional properties of protein-polysaccharide complexes: A review. In *Critical*
592 *Reviews in Food Science and Nutrition*, 38 (8), 689-753.
- 593 Shimazaki, K.-I., Kawano, N., & Yoo, Y. C. (1991). Comparison of bovine, sheep and goat
594 milk lactoferrins in their electrophoretic behaviour, conformation, immunochemical
595 properties and lectin reactivity. *Comparative Biochemistry and Physiology Part B:*
596 *Comparative Biochemistry*, 98(2-3), 417-422.
- 597 Souillac, P. O., Middaugh, C. R., & Rytting, J. H. (2002). Investigation of
598 protein/carbohydrate interactions in the dried state. 2. Diffuse reflectance FTIR studies.
599 *International Journal of Pharmaceutics*, 235, 207-218.
- 600 Steijns, J., Brummer, R. J., Troost, F. J., & Saris, W. H. (2001). Gastric digestion of bovine
601 lactoferrin in vivo in adults. *The Journal of nutrition*, 131 (8), 2101-2104.
- 602 Stogov, S. V., Izumrudov, V. A., & Muronetz, V. I. (2010). Structural changes of a protein
603 bound to a polyelectrolyte depend on the hydrophobicity and polymerization degree of the
604 polyelectrolyte. *Biochemistry (Moscow)*, 75(4), 437-442.
- 605 Tolstoguzov, V. B. (1991). Functional properties of food proteins and role of protein-
606 polysaccharide interaction. *Food Hydrocolloids*, 4(6), 429-468.
- 607 Turgeon, S. L., Schmitt, C., & Sanchez, C. (2007). Protein-polysaccharide complexes and
608 coacervates. *Current Opinion in Colloid & Interface Science*, 12(4-5), 166-178.
- 609 Ueno, H., Ueda, N., Morita, M., Kakehi, Y., & Kobayashi, T. (2012). Thermal stability of the
610 iron-lactoferrin complex in aqueous solution is improved by soluble soybean polysaccharide.
611 *Food biophysics*, 7 (3), 183-189.
- 612 Vinayahan, T., Williams, P. A., & Phillips, G. O. (2010). Electrostatic interaction and
613 complex formation between gum arabic and bovine serum albumin. *Biomacromolecules*, 11
614 (12), 3367-3374.
- 615 Vold, I. M. N., Kristiansen, K. A., & Christensen, B. E. (2006). A study of the chain stiffness
616 and extension of alginates, in vitro epimerized alginates, and periodate-oxidized alginates

- 617 using size-exclusion chromatography combined with light scattering and viscosity detectors
618 *Biomacromolecules*, 7 (7), 2136-2146.
- 619 Vold, I. M. N., Kristiansen, K. A., & Christensen, B. E. (2007). A study of the chain stiffness
620 and extension of alginates, in vitro epimerized alginates, and periodate-oxidized alginates
621 using size-exclusion chromatography combined with light scattering and viscosity detectors
622 *Biomacromolecules*, 8, 2627.
- 623 Wells, L. A., & H. Sheardown (2007). Extended release of high pI proteins from alginate
624 microspheres via a novel encapsulation technique. *European Journal of Pharmaceutics and*
625 *Biopharmaceutics*, 65(3), 329-335.
- 626 Xu, Y., Mazzawi, M., Chen, K., Sun, L., & Dubin, P. L. (2011). Protein purification by
627 polyelectrolyte coacervation: Influence of protein charge anisotropy on selectivity.
628 *Biomacromolecules*, 12 (5), 1512-1522.
- 629 Ye, A. (2008). Complexation between milk proteins and polysaccharides via electrostatic
630 interaction: principles and applications – a review. *International Journal of Food Science and*
631 *Technology*, 43, 406-415.
- 632 Ye, A. Q., & Singh, H. (2007). Formation of multilayers at the interface of oil-in-water
633 emulsion via interactions between lactoferrin and beta-lactoglobulin. *Food biophysics*, 2(4),
634 125-132.
- 635 Zhao, Y., Li, F., Carvajal, M. T., & Harris, M. T. (2009). Interactions between bovine serum
636 albumin and alginate: An evaluation of alginate as protein carrier. *Journal of Colloid and*
637 *Interface Science*, 332(2), 345-353.

Caption for table supplied:

Table 1

Thermal denaturation temperatures (T_{\max}) and enthalpy change of denaturation (ΔH_{cal}) of Lf samples and Lf-alginate mixtures (1:1) (10% w/w).

ACCEPTED MANUSCRIPT

Table:

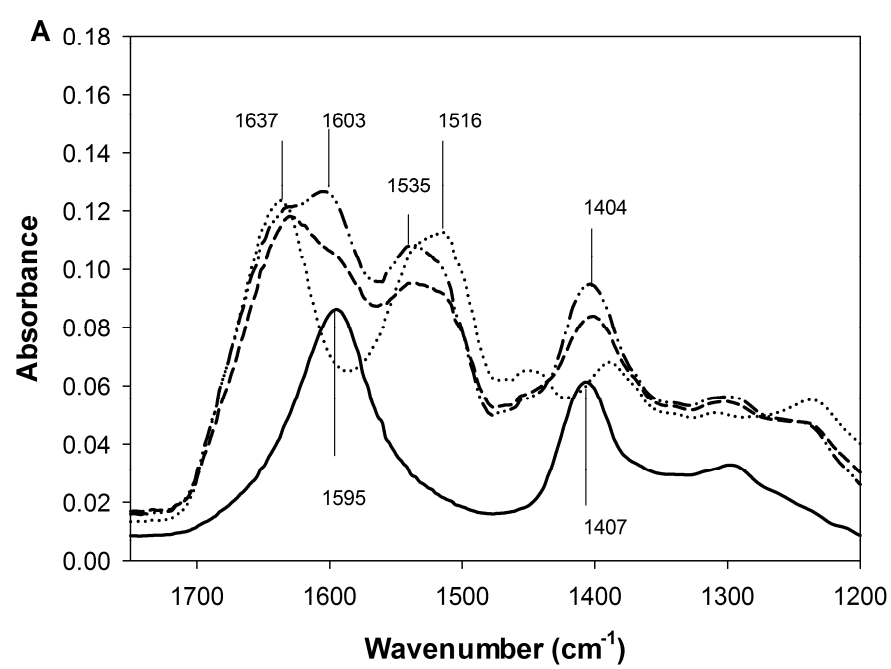
Table 1

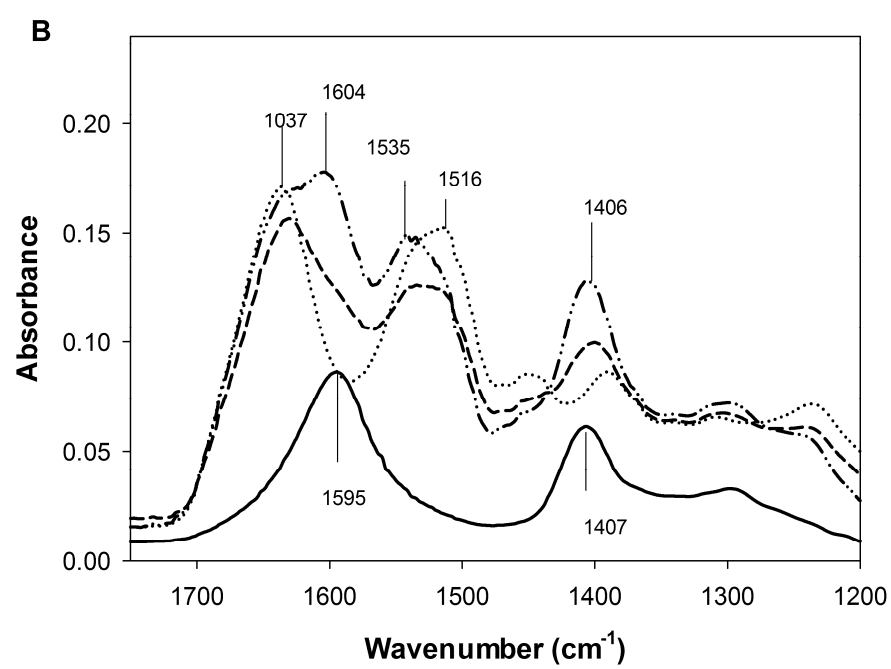
Sample	Peak 1: $T_{\max 1}$ (°C)	$\Delta H_{\text{cal 1}}$ (J/g)	Peak 2: $T_{\max 2}$ (°C)	$\Delta H_{\text{cal 2}}$ (J/g)
Apo-Lf	70.7 ± 0.8^c	13.2 ± 0.2^C	-	-
Mixture (Apo-Lf)	69 ± 1^{cd}	8.1 ± 0.8^D	-	-
Native-Lf	60.5 ± 0.5^e	14 ± 1^{BC}	89.2 ± 0.5^b	2.0 ± 0.1^E
Mixture (Native-Lf)	67 ± 1^d	7.3 ± 0.7^D	88 ± 2^b	1.0 ± 0.1^E
Holo-Lf	-	-	91.3 ± 0.5^b	21.0 ± 0.6^A
Mixture (Holo-Lf)	-	-	94.2 ± 0.4^a	15.3 ± 0.9^B

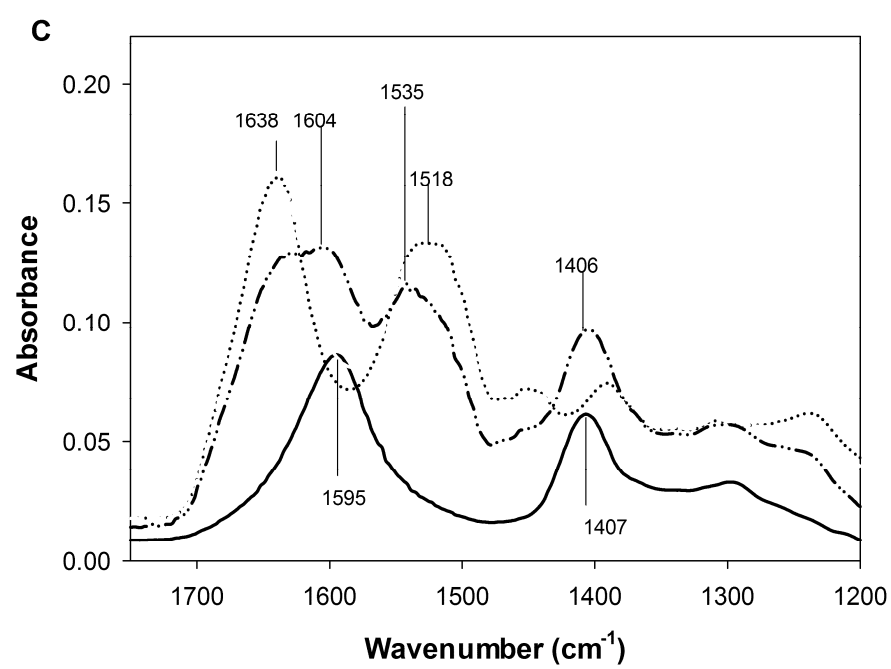
Mean values of T_{\max} and ΔH_{cal} (vertical column) that do not share a letter are significantly different at $P < 0.05$.

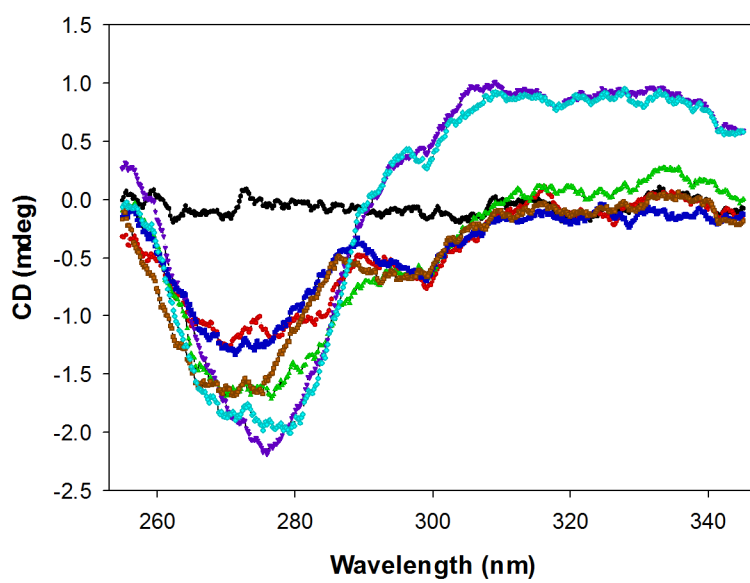
Captions for Figures supplied:

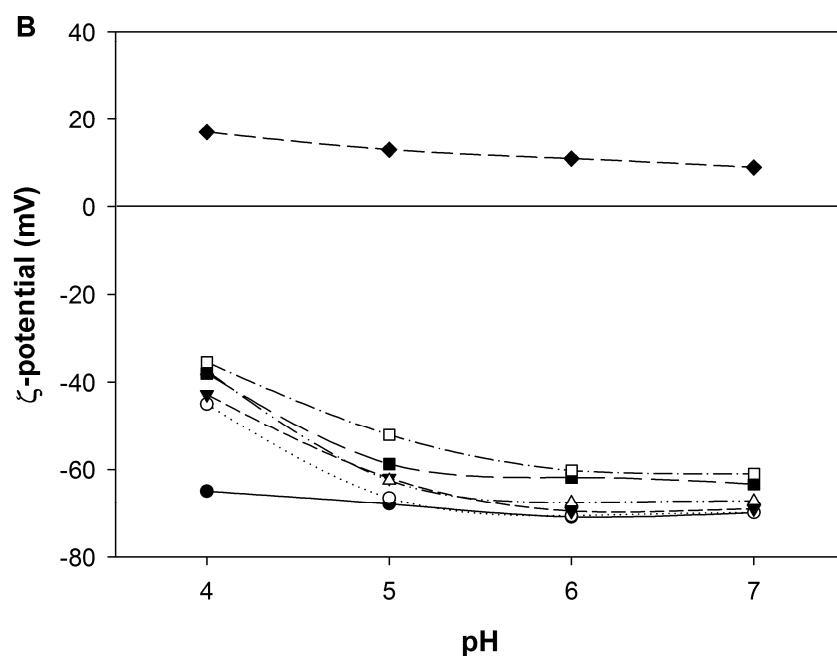
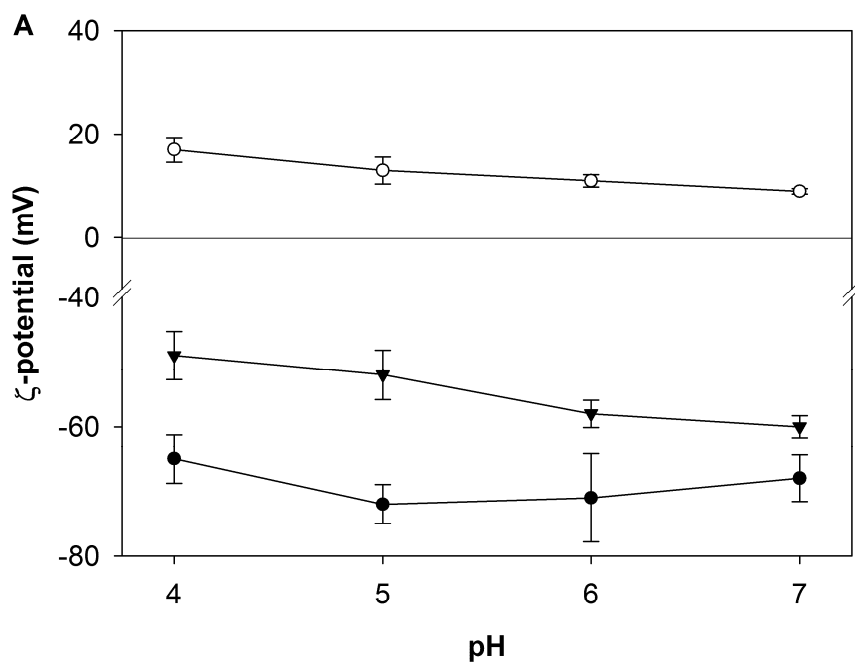
Figure	Caption	Remarks/Format
Fig. 1	<p>FTIR spectra of alginate, different forms of Lf and their respective mixtures (Lf-alginate = 1:1); dry mixed & freeze dried mixture in the wavelength region 1750–1000 cm^{-1}.</p> <p>(A) Apo-Lf and its mixtures, (B) Native-Lf and its mixtures and (C) Holo-Lf and its mixtures.</p> <p>Alginate (—), Lf (⋯), dry mixed mixtures (---) and freeze dried mixtures (----). As holo-Lf was not able to form homogenous mixture when dry mixed, the spectrum has been removed.</p>	TIFF
Fig. 2	<p>Circular dichroism spectra of alginate (●, black), apo-Lf (○, red), native-Lf (Δ, green), holo-Lf (∇, violet), MA (■, navy blue), MN (□, brown), MH (◇, blue) in aqueous solution. M represents mixtures of alginate & Lf (1:1) where A (apo-), N (native-) & H (holo-) Lf.</p>	TIFF
Fig. 3	<p>(A) The zeta-potential values of native-Lf (○), alginate (●) and Lf-alginate mixtures at 1:1 ratio (▼) in pH range 4.0 – 7.0 (1 mM KCl);</p> <p>(B) Zeta-potential values of native-Lf-alginate mixture at different mixing ratios at pH 4-7 (1 mM KCl). Lf (◆), Alg (●), Alg:Lf=9:1 (○), Alg:Lf=8:2 (▼), Alg:Lf=7:3 (Δ), Alg:Lf=6:4 (■) & Alg:Lf=5:5 (□);</p> <p>(C) The zeta-potential of apo-, native- and holo-Lf and their alginate mixtures at 1:1 ratio at pH 4 and 7;</p> <p>(D) The zeta-potential of apo-, native- and holo-Lf and their alginate mixtures at natural pH in mixing ratios of 1:1 (ie. 5:5) and 1:1.5 (ie. 4:6).</p>	TIFF
Fig. 4	<p>(A) Native-PAGE of Native-Lf and its mixture with alginate (MN) in different mixing ratios (alginate: native-lf);</p> <p>(B) Native-PAGE of different forms of Lf (apo-, native & holo-) and their mixtures (MA, MN & MH) in equal mixing ratio (1:1) at different storage days (0, 1 & 7). The values from the densitometer analysis (relative amount of Lf migrated from the mixture) are given at the bottom of the gels.</p>	The figures are the original gels scanned using Gel Densitometer (GS-800). Thus is saved in JPEG format, as converting them to TIFF led to fading of bands.
Fig. 5	<p>(A) Comparison of apparent viscosities at shear rate 25 s^{-1} of mixtures of alginate and Lf [apo-(A), native-(N), Lf-50 & holo-(H)] at different ratios (alginate:Lf of 3:1, 1:1, 1:1.5 & 1:3) at natural pH;</p> <p>(B) % Contribution of Lf to viscosity increase of these mixtures as calculated from equation 1.</p>	TIFF

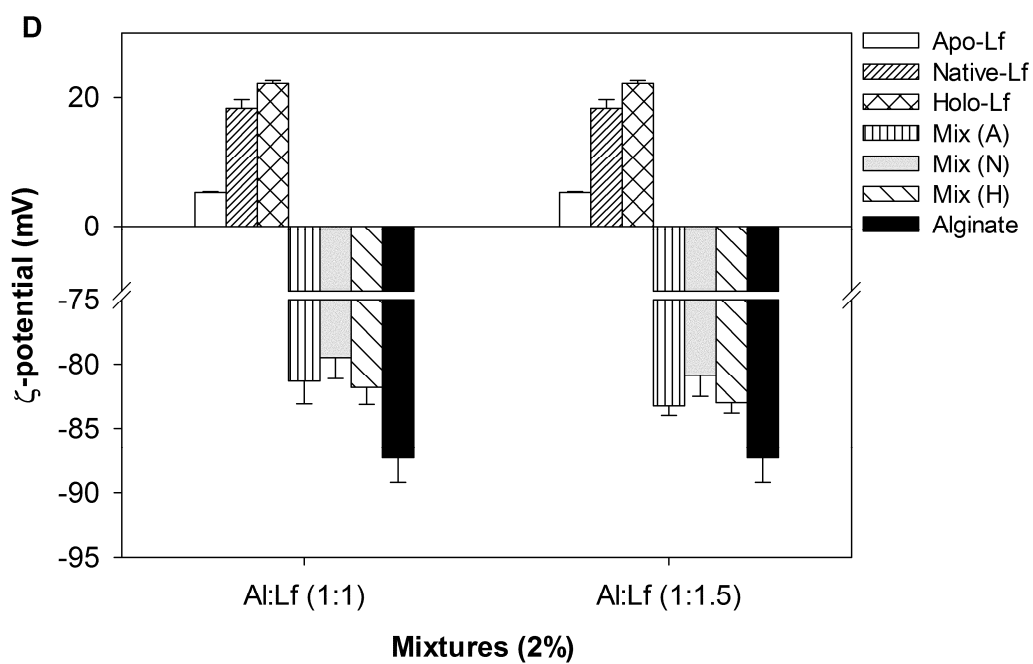
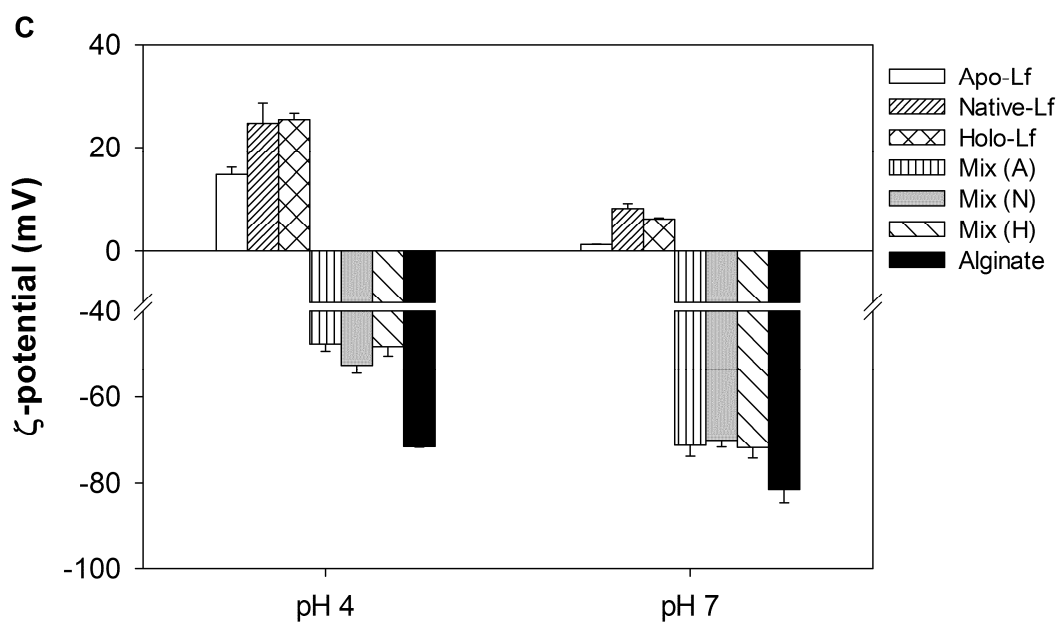


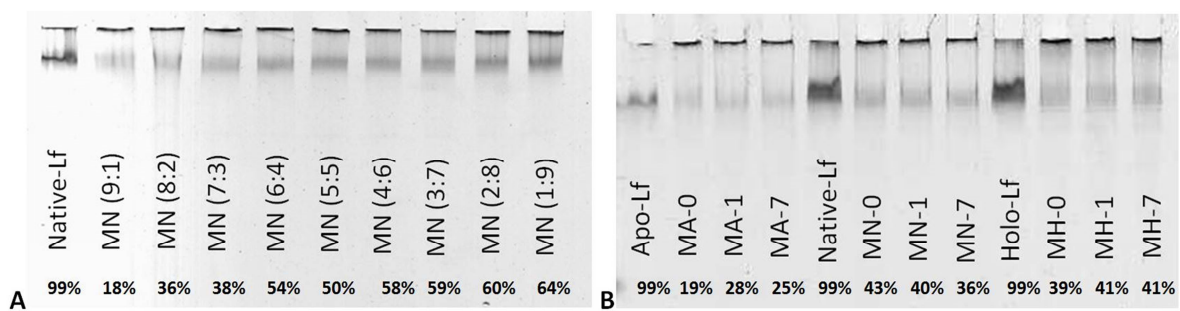


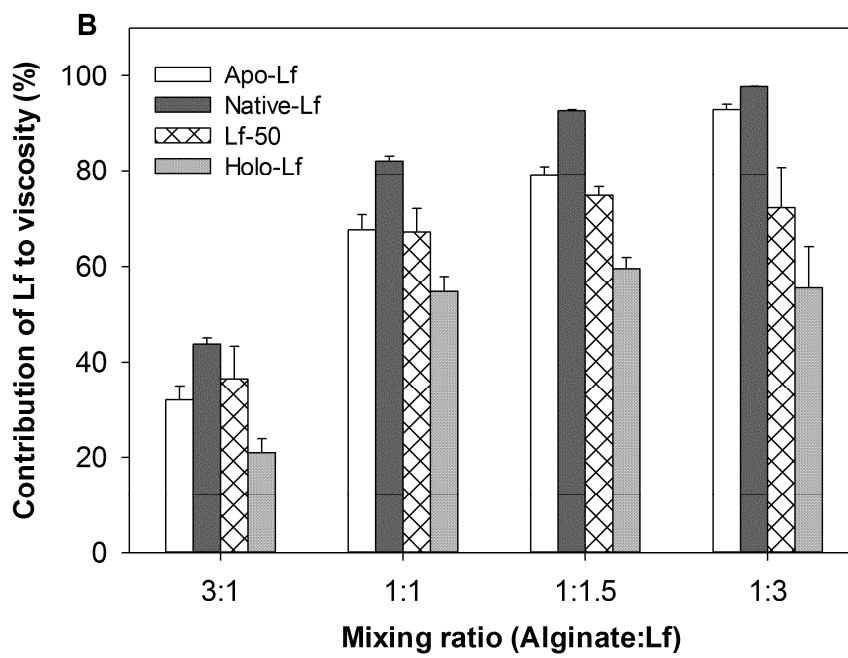
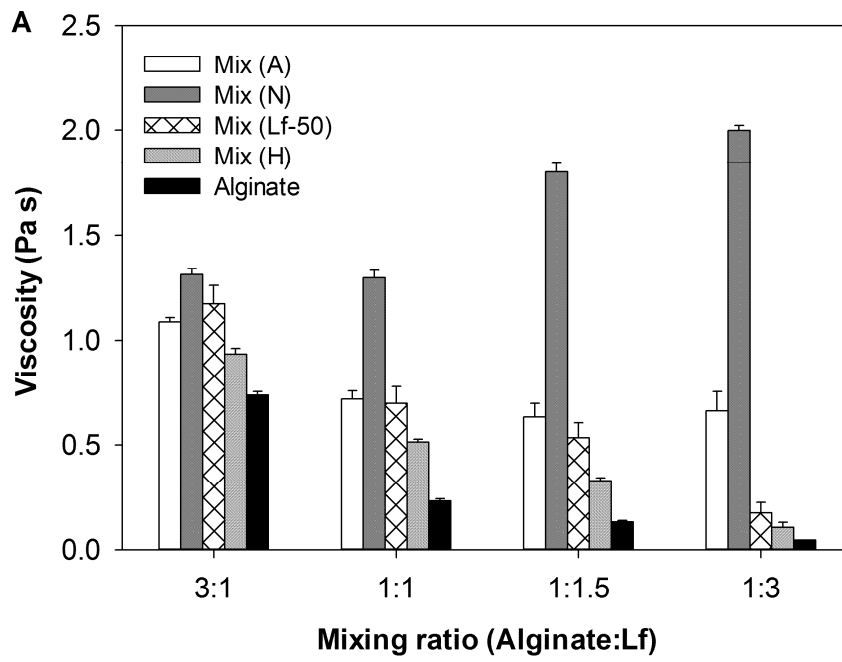






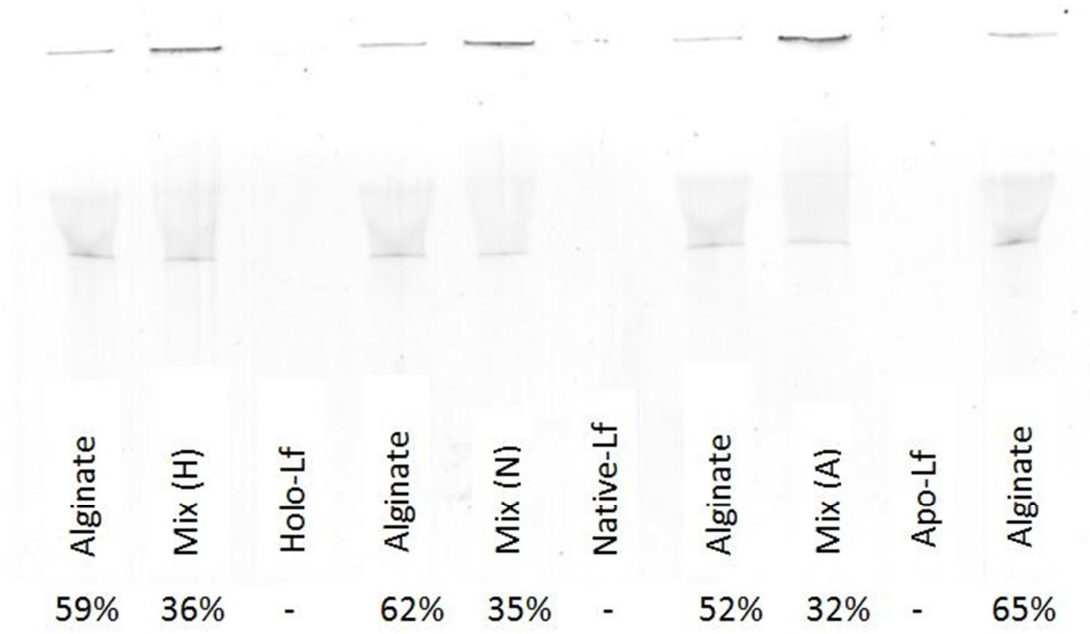






Highlights:

1. All forms of Lactoferrin (Lf) retain their structural conformation in Lf-alginate mixtures.
2. Molecular interactions between Lf and alginate involve the alginate carboxylate groups.
3. Native-PAGE was used to evaluate the binding capacity of alginate towards Lf.
4. All forms of Lf contribute to an increase in viscosity of Lf-alginate mixtures.



ACCEPTED MANUSCRIPT